Vol. 86 No. 3 pp. 608–618 ACTA GEOLOGICA SINICA (English Edition) June 2012

The Genesis Mechanism of the Mantle Fluid Action and Evolution in the Ore-Forming Process: A Case Study of the Laowangzhai Gold Deposit in Yunnan, China

LIU Xianfan[1, 2, *], LI Chunhui[1], LU Qiuxia[1], DENG Biping[1], SONG Xiangfeng[1], ZHAO Fufeng[1], CHU Yating[1], XIAO Jixiong[1], YI Liwen[1] and HUANG Yupeng[1]

1 *Institute of Earth Science, Chengdu University of Technology, Chengdu 610059, China*
2 *State Key Laboratories for Mineral Deposits Research, Nanjing University, Nanjing 210093, China*

Abstract: Based on petrological studies of the wall rocks, mineralizing rocks, ores and veins from the Laowangzhai gold deposit, it is discovered that along with the development of silication, carbonation and sulfidation, a kind of black opaque ultra-microlite material runs through the spaces between grains, fissures and cleavages. Under observations of the electron microprobe, scanning electronic microscopy and energy spectrum, this kind of ultra-microlite material is confirmed to consist of ultra microcrystalline quartz, silicate, sulfides and carbonates, as well as rutile, scheelite and specularite (magnetite), showing characters of liquation by the analyses of SEM and energy spectrum. The coexistence of immiscibility and precipitating co-crystallization strongly suggests that the mineralizing fluid changed from the melt to the hydrothermal fluid. Combined with the element geochemical researches, it is realized that the ultra-microlite aggregate is the direct relics of the mantle fluid behaving like a melt and supercritical fluid, which goes along with the mantle-derived magma and will escape from the magma body at a proper time. During the alteration process, the nature of the mantle fluid changed and it is mixed with the crustal fluid, which are favorable for mineralization in the Loawangzhai gold deposit.

Key words: micro-petrography, black opaque material, ultra-microlite aggregate, mantle fluid process and evolution, the Laowangzhai gold deposit

1 Introduction

The Laowangzhai gold deposit is located in Zhenyuan County of Yunnan Province, southwestern China. Since it was discovered in the 1980s, many geologists have carried out researches on the genesis of the deposit, but failed to arrive at a unanimous and receivable conclusion. With regard to the most disputed topic, the source of the mineralizing fluid, several hypothesizes are proposed, e.g., the volcanic fluid (Hu and Tang, 1995), the metamorphic fluid (Tang et al., 1991), the magmatic fluid (He, 1993), the tectonic metasomatic fluid (Xue, 2002) as well as the fluid produced by mantle degassing process (He and Hu, 1996; Huang and Liu, 1999). Based on the researches of fluid inclusions from Au-bearing quartz veins, Liang et al. (2011) argued that the ore-forming fluid from the Laowangzhai gold deposit is a product of mantle-derived fluids and its geologic features are similar to those of the Himalayan collision orogenic gold deposits. Although opinions are different, it is accepted that the mineralizing fluid is closely connected to the deep geological processes. The following questions are proposed: (1) where did the mineralizing fluid come from, the deep crust or the mantle? (2) How did the mineralizing fluid behave: did the deep fluid provide the mineralizing materials directly or the crustal materials were activated by the deep fluid? Based on the petrological and element geochemical studies, the relationship between the black opaque ultra-microlite material from altered lamprophyre and the mineralization is discussed.

* Corresponding author. E-mail: liuxianfan@cdut.cn

2 Regional Geologic Setting

Tectonically, the research area is located in the Ailaoshan Mountain tectonic-magmatic-metamorphic zone sandwiched between the Honghe River, Ailaoshan Mountain (Cao et al., 2010; Chen et al., 2010) and the

Jiujia-Mojiang deep faults, and is an important gold belt in the Sanjiang River orogen. The Laowangzhai gold deposit is situated at the hanging wall of the Jiujia-Mojiang fault, consisting of the Lannitang, Donggualin, Laowangzhai, Daqiaoqing and Kudumu ore blocks from northwest to southeast. The main attention is paid to the Laowangzhai and Donggualin ore blocks in this research. Sedimentary rocks in the two ore blocks are composed of sericite slate, metamorphosed quartz greywacke and carbonaceous radiolarian siliceous rocks from the Devonian, lamellar carbonaceous marl and siliceous sericite slate from the Carboniferous a red siltstone from the Triassic System. Igneous rocks in this area, including lamprophyre, altered ultrabasic rocks, altered basalt and quartz porphyry, are well studied, but their relationship to gold mineralization is still in question. The Laowangzhai gold deposit is well controlled by a suite of faults which consist of northwest first-grade faults, northwest-west second-grade faults and northeast third-grade faults.

The three deep faults (Honghe River Fault, Ailaoshan Mountain Fault and Jiujia-Mojiang Fault) are active in a long geologic history with high development of tectonic-magma-fluid activities. During the late Paleozoic Era, pull-apart and fault depression were the main tectonic movements in this region. From late Variscan to Indosinian the compressional movement predominated, while in the Yanshanian, it was converted to pull-apart again, and during the Himalayan thrusting movement became the main tectonic form, entering the collision orogenic process. The collision orogenic process can be divided into three stages, the main collision stage (65-41 Ma), the late collision stage (40-26 Ma) and the post-collision stage (26 Ma-present) (Hao et al., 2005; Hou et al., 2006). During the late collision stage, metallogenesis was intensive, especially near the tectonic node in the eastern Himalayas, and most of the gold deposits in the Ailaoshan belt were related to the ductile shear structures. Based on the above analysis, it is recognized that the Laowangzhai gold deposit was formed during the intracontinental tectonic transformation stage, controlled by strike-slip, nappe and ductile shear structures, and subjected to mantle upwelling, magmatism and deep fluid activity.

3 Ore Geology Description

The Laowangzhai and Donggualin ore blocks are composed of ultrabasic and basic volcanic rocks (the former) and lamprophyre and quartz porphyry (the latter) respectively, and mainly controlled by both the Carboniferous System and the northwest structures and paleovolcanos (Fig. 1).

The main ore bodies in the two ore blocks are in the shape of layers, bandings, lenticles and veins, while the ore bodies along the faults appear in branches and swarms. Late Hercynian-Indosinian rocks are well developed, e.g. peridotite, pyroxene peridotite, olivine pyroxenite and pyroxenite (Liang et al., 2011). Quartz porphyry can be seen as veins. Basic lavas and lamprophyres are closely related to the ore-forming process (Ren et al., 1995). The former are mainly composed of dolerite and vitrobasalt. The lamprophyric rocks occur in veins and are dominated by minette which is composed of biotite (phenocryst)+ pyroxene (phenocrysts, a few) + potash feldspar + plagioclase. Some biotite phenocrysts have been replaced by bissolithe. In the cleavages of biotite and spaces between bissolithe grains, black opaque materials (BOM) are developed as veinlets and speckles with the appearances of silicon alkaline alteration such as plagioclase and quartz. The BOM can be found in all the altered rocks which are connected to ores. Au occurs as native gold, Ag-bearing native gold and electrum. The metal minerals include pyrite and arsenopyrite, while nonmetallic minerals are predominantly ankerite, sericite, siderite and feldspar. The ore types consist mainly of the altered rock type and the quartz vein type (Lü, 1994, Bian, 1998, Ying and Liu, 2000), and there are still other ore types such as the altered slate type, the metamorphic quartz greywacke as well as the brown hematite type (Lü et al., 1994; Bian et al., 1998, Ying and Liu, 2000). The primary ore textures include the cataclastic, enlarged atoll, metasomatic and wrapping ones; the ore structures are dominated by laminated, brecciform and network-veinlet ones.

Serpentinization, chloritization, sericitization, silication, carbonation and sulfidization are well developed, in which the silication, carbonation and sulfidization are poly-staged and closely related to the gold mineralization. Based on the alteration features and mineral paragenesis, four mineralization stages have been recognized (Ying and Liu, 2000): in the first stage scheelite-quartz formed with minor gold; in the second stage carbonation, silication and sericitization developed and native pyrite-arsenopyrite formed; in the third stage carbonation developed and native gold-pyrite-stibnite formed; and in the last stage quartz and calcite formed with little gold mineralization.

Numerous researches have indicated that gold mineralization in the Laowangzhai gold deposit is related to the lamprophyres, as both were formed in the Himalayan Period (Tang et al., 1991; Wang et al., 2001), and lamprophyre-type gold deposits account for almost 50% of the gold reserves in the Donggualin ore block. Huang et al. (1996, 1997) suggested that these lamprophyres were derived from the metasomatized enriched mantle and affected by the slab fluid which was high in $^{87}Sr/^{86}Sr$ and low in $^{143}Nd/^{144}Nd$. According to the

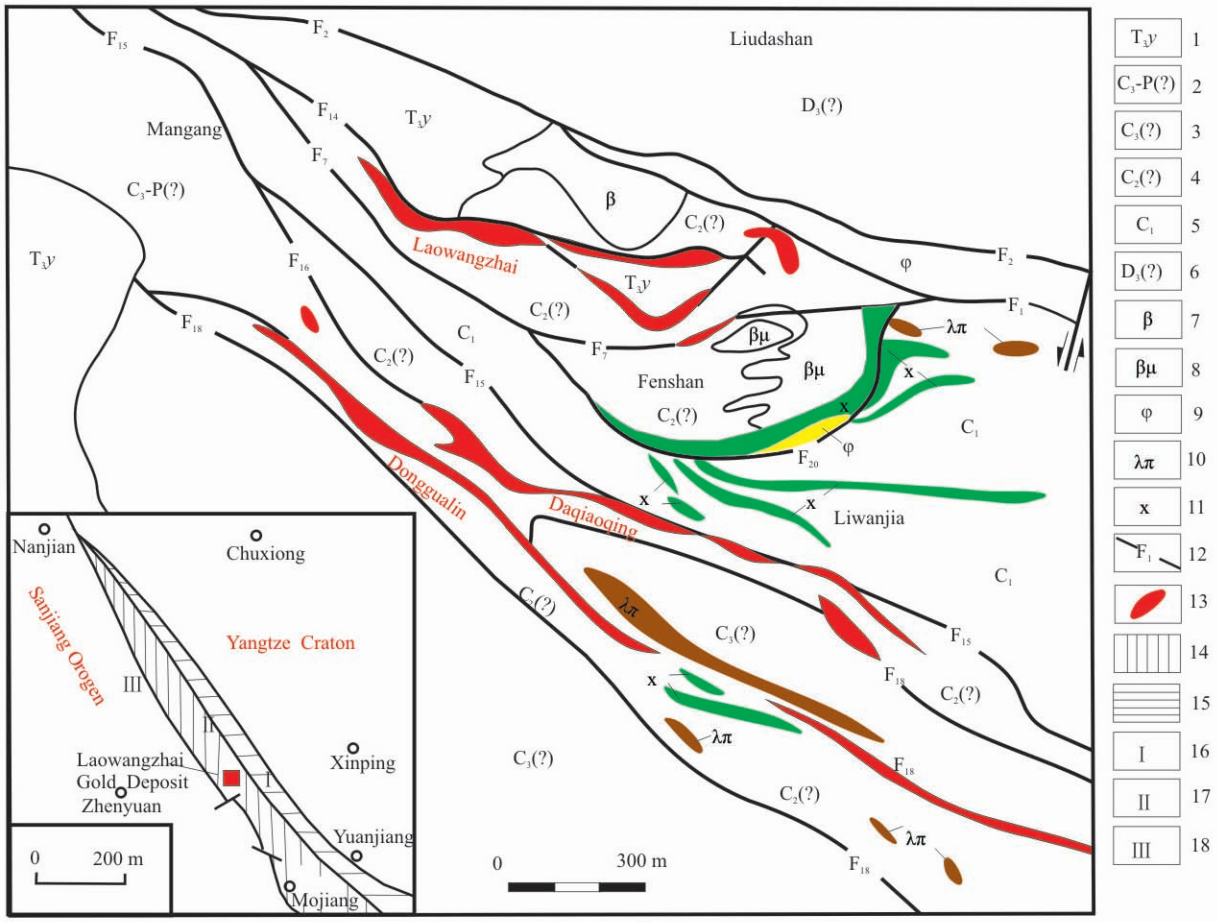

Fig. 1. Geological sketch map of the Laowangzhai gold deposit (After Ren et al., 1995 and Huang et al., 1996).
1. Mudstone, sandstone and glutenite of the upper Triassic Yiwanshui Formation; 2. metamorphosed fine quartz graywacke and glutenite intercalated with didrimit slate of the upper Carboniferous. Permian packing; 3. quartz graywacke intercalated with didrimit slate of the upper Carboniferous; 4. metamorphosed quartz graywacke intercalated with didrimit slate and silicalite of the middle Carboniferous; 5. carbonaceous-argillaceous limestone intercalated with carbonaceous-calcareous slate of the lower Carboniferous; 6. gray flaggy metamorphosed quartz graywacke intercalated with sandy-didrimit slate of the upper Devonian; 7. basalt; 8. mimesite; 9. hyperbasite; 10. quartzophyre; 11. lamprophyre; 12. fault and number; 13. mineralization; 14. epimetamorphic belt; 15. metamorphic bathozone; 16. Red River fault zone; 17. Ailaoshan fault zone; 18. Jiujia-Mojiang fault zone.

PGE geochemistry of the lamprophyre, Wang et al. (2001) suggested that Au was enriched later. It is argued that the lamprophyre itself cannot provide ore-forming materials, especially gold, and the ore-forming fluid should be the mantle fluid derived from the enriched mantle during the mantle degassing process (Li et al., 1995; Huang et al., 1996, 2001; Ying and Liu, 2000; Ding et al., 2001; Zhang et al., 2010).

4 Petrography of Rocks and Ores

Rocks and ores in the Laowangzhai gold deposit are various, including the altered quartz porphyry, altered quartz sandstone, serpentinized-carbonated ultrabasic rocks (pyroxene peridotite, olivine pyroxenite, pyroxenite and Canaanite), altered lamprophyre and altered didrimit slate-phyllite gold ores. The petrographic features are illustrated in Fig. 2.

The matrix of quartz porphyry from the Dongqualin ore block is mainly composed of fine-grained quartz (seemingly related to silication) with sericite distributed homogeneously, cut by carbonate veinlets and overprinted by fine-grained pyrite and acicular stibnite (Fig. 2a). As exhibited in Fig. 2b, carbonation in the altered quartz sandstone is overprinted by metalliferous mineralization, while in the pyroxene peridotite and olivine pyroxenite, serpentinization was overprinted by carbonation. When the temperature is higher than 300° C, olivine and pyroxene will be replaced by radiating moissanite on the one hand, and on the other hand, their margins or fissures will be filled with carbonates; if the temperature is lower, quartz will be released and the silicated quartz will be contained in the carbonates veins (Fig. 2c).

Porphyritic bistagite, also the diopside, were cut by multi-stage carbonate veinlets containing microcrystalline quartz (Fig. 2d), which implies that early-stage alterations

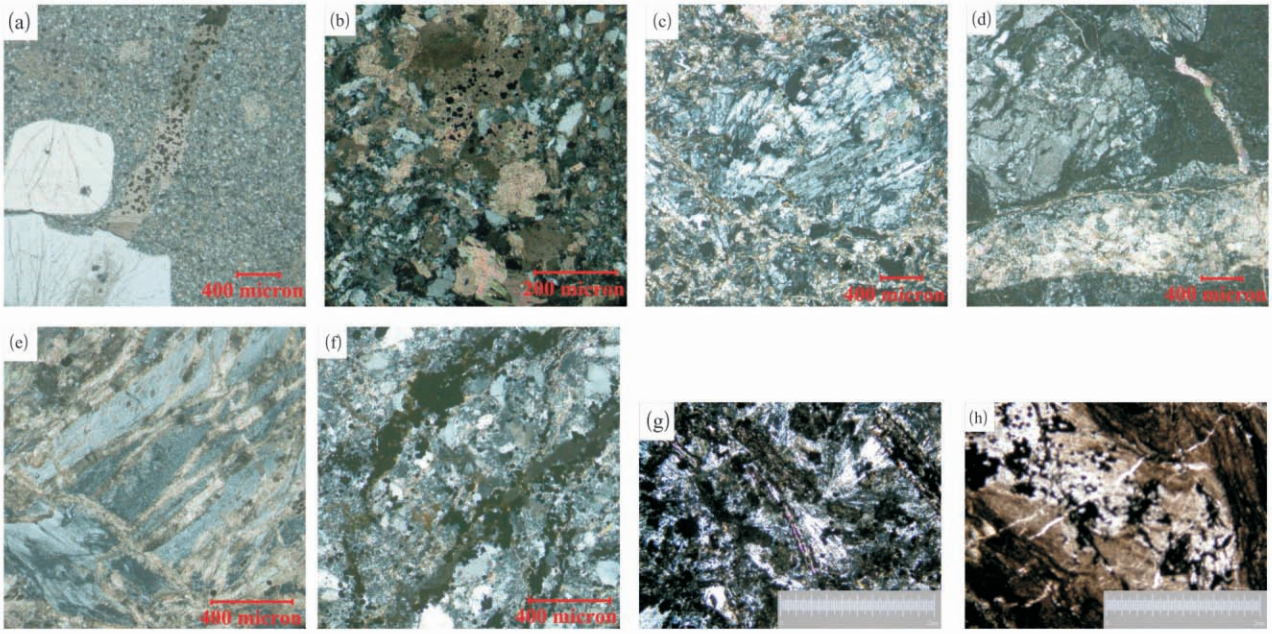

Fig. 2. Microscopic features of the alterated rocks in the Laowangzhai gold deposit.
(a) to (g), crossed polarized light in penetration of light; (h), plainlight in penetration of light: (a), mineralized-altered quartzophyre: carbonatized veinlet superimposing mineralization of sulfide in microlithic matrix (Donggualin ore block); (b), slightly mineralized-altered feldspar quartz sandstone: accompanying carbonatization and superimposing mineralization of sulfide (Donggualin ore block); (c) , carbonatized and grammite-formed pyrolite: accompanying strong carbonatization and grammite-formation, radiated grammite replacing originally mineral grains (Donggualin ore block); (d), silicated and carbonatized porphyritic-like bistagite, one carbonate vein bearing microlite quartz cutting phenocrystic malacolite and microlitic matrix, and another carbonate vein cutting phenocryste, matrix and the former carbonate (Laowangzhai ore block); (e), silicated and carbonatized gold ore, finely crystallized carbonate alternates orientatedly with cryptocrystallized-mirolitic as band and undulatory extinction, which indicates that intense orientated stress accompanies the mineralization and alteration process (Laowangzhai ore block); (f), mineralized and altered silicinate quartzose sandstone, the mineralization mainly overprints the microlitic and finely silicated portions (Laowangzhai ore block); (g), altered lamprophyre, primitive biotite (sheet), metasomatic microciline (radical, bluish gray-white), bissolithe (columnatic and acicular, dark green) and BOM as inhomogeneous nodules adherent to amphibole (Donggualin ore block); (h), altered pinal slate-phyllite: silicated veins and BOM as nodules and veinlets (Donggualin ore block).

were overprinted by later ones. As shown in Fig. 2e, striped microcrystalline carbonates and quartz veinlets show wavy extinction, suggesting that the alteration and mineralization processes were affected by oriented tectonic stresses. While in the altered quartz sandstone, later metal mineralization mainly overprinted the microcrystalline quartz veinlets (Fig. 2f).

However, special attention should be paid to the altered lamprophryre, radial felsic minerals and acicular alkaline amphiboles which are overlapped by the BOM (Fig. 2g). Silicated quartz veinlets from altered sericite slate also contain the BOM (Fig. 2h). Their optical characteristics under the reflected light imply that they are not carbonaceous, ferruginous or sulfides. Analyses of EPM, SEM and energy spectrum indicate that the BOM is closely related to mineralization and alteration, and it may be a new window to look into the deep geological processes.

5 Compositions and Nature of the BOM

5.1 Characteristics and compositions of the BOM

Results of an EPM analysis of the BOM from altered lamprophyre are listed in Table 1, while data of the energy spectrum analysis are listed in Table 2 in correspondence to Fig. 3. From the data and images exhibited, the following conclusions can be drawn .

(1) As shown in Fig. 3, the coexistence of immiscibility and precipitating cocrystallization textures from the BOM (diameter≤6 μm, mostly 2–4 μm) implies that the ore-forming fluid has changed in nature, which is reflected by the fact that scheelite was exsolved from rutile (Fig. 3a), a precipitating cocrystallization texture was formed between dolomite and rutile (Fig. 3a), and between arsenopyrite and microcline (Fig. 3b); an exsolution texture was shown by rutile being exsolved from specularite (Fig. 3d) and scheelite being exsolved from rutile again (Fig. 3d), and also the unique association of pyrite and anhydrite (Fig. 3c). Drawn from the above analysis, the BOM is a kind of microcrystalline-cryptocrystalline matter composed of silicates, carbonates and sulfides, and rich in Fe, W, and Ti. The coexistence of immiscibility and precipitating co-crystallization suggests that the BOM-forming fluid changed from a melt to a hydrothermal fluid. When the environment changed from reducing to oxidizing, S^{2-} was converted to S^{6+} (pyrite→anhydrite). Combining the dual immiscibility of the BOM (Fig. 3d) and the scheelite-bearing quartz veinlets in the field, it is argued that the

Table 1 Electron microprobe analyses of the BOM aggregate from altered lamprophyre (DGL-02) in the Donggualin ore block (wt%)

Measuring spot	Sample No.	SiO_2	TiO_2	AL_2O_3	FeO	MnO	MgO	CaO	Na_2O	K_2O	Cr_2O_3	Total	Mineral
1	DGL02-1①	65.79	0.06	18.64	0.24	0.02	0.00	0.25	2.00	12.61	0.02	99.63	Microcline
2	DGL02-4	65.85	0.05	19.41	0.48	-	0.00	0.22	0.64	13.41	0.03	100.09	Microcline
3	DGL02-6	63.60	0.01	18.59	0.22	0.01	0.06	0.01	0.19	16.04	0.01	98.74	Microcline
4	DGL02-5	97.55	0.05	0.43	0.27	0.02	0.41	0.53	-	0.04	-	99.30	Quartz
5	DGL02-3③	0.75	0.13	0.33	2.41	0.57	19.79	32.69	0.25	0.14	0.06	57.12	Dolomite
6	DGL02-7③	1.43	0.03	0.09	3.77	0.64	15.40	26.47	0.42	0.09	0.02	48.36	Dolomite
7	DGL02-2④	1.19	0.04	0.26	0.30	0.06	0.23	51.80	0.24	0.35	0.02	54.49	Calcite

Notes: Needle-shaped minerals ① and green slaty minerals ④ in Fig. 2G; major component CO_2 is absent in ②, ③ and ④.
Data tested by Zheng Shu from the EMP center of the State Key Laboratory of Geological Processes and Mineral Resources, China University of Geosciences; instrument used: JXA-8100, working voltage: 15kV, working electric current: 20 Na, probing spot diameter: 1μm±.

Table 2 Energy spectrum analysis of the BOM aggregate from altered lamprophyre (DGL-02) in the Donggualin ore block

Measuring spot		Ti	Ca	Mg	Al	Si	W	K	Fe	C	As	S	O	Total	Mineral
1	wt%	46.02	1.05										52.93	100	rutile
	X_B%	22.37	0.61										77.02	100	
2	wt%	39.74	1.01				11.51		2.81				44.93	100	tungstiferous
	X_B%	21.97	0.67				1.66		1.33				74.37	100	rutile
3	wt%		11.98				52.61						35.41	100	scheelite
	X_B%		10.68				10.22						79.1	100	
4	wt%		13.39	7.64						33.93			45.04	100	dolomite
	X_B%		5.31	5						44.92			44.77	100	
5	wt%								31.02		43.64	25.35		100	arsenopyrite
	X_B%								28.8		30.2	41		100	
6	wt%				8.42	26.32		11.04					54.22	100	microcline
	X_B%				6.34	19.05		5.74					68.87	100	
7	wt%								41.88			58.12		100	pyrite
	X_B%								29.26			70.74		100	
8	wt%		15.77	0.78								18.2	65.24	100	anhydrite
	X_B%		7.76	0.64								11.2	80.41	100	
9	wt%								64.28				35.72	100	specularite
	X_B%								34.02				65.98	100	
10	wt%	46.16										0.98	52.86	100	rutile
	X_B%	22.42										0.71	76.87	100	

Note: Tested by Xu Jinsha at the Energy Spectrum Center of Chengdu Institute of Geology and Mineral Resources; instrument used: Hitachi-4800, Oxford Energy Spectrum 250, probing spot diameter 4 μm±.

ore-forming mantle fluid was overlapped by the crustal fluid related to the wolfram-forming granitic magma.

(2) Although the energy spectrum analysis is semiquantitative, minerals of simple compositions can be determined. And, for the silicates with clear composition ratios, this analysis is also useful. The data listed in Table 2 and Table 1 is basically concordant. It can be deduced from Table 2 that CO_2 data are mainly absent in the measuring spots 5–7 in Table 1.

(3) As observed from Figs. 2g and 2h, the BOM is related to silication and alkaline metasomatism. A comparison between Table 1 and Table 2 indicates that the compositions of BOM are similar to those of the alteration types (silication, carbonation and sulfidation), which implies that the BOM-forming fluid was independent of lamprophyre magma and could trigger off mineralization. Then, what is the nature of this BOM-forming fluid?

5.2 Discussion on the nature of the BOM

(1) Crystalline, cryptocrystalline, microcrystalline or non-crystalline?

It is well known that carbonaceous or metal materials, black glass or transparent mineral crystals with diameters smaller than 10 μm will be black and opaque under the optical microscopes. Based on Fig. 3 and Tables 1 and 2, it is convinced that the BOM is predominantly composed of crystalline silicates and carbonates with unclear crystal shapes, as well as rutile, sulfides and specularite. Rutile appears in two ways, the one is precipitating with carbonates, and the other is non-immixing with specularite. Therefore, the BOM is an ultra-microcrystalline aggregate, rather than a carbonaceous or metal material or black glass.

(2) A melt or a hydrothermal fluid?

The occurrence of the BOM from altered lamprophyre and sericite slate-phyllite indicates that the BOM-forming fluid is different from the hydrothermal fluid. (a) The compositions of the BOM suggest that it is an intermixture of silicates, carbonates, sulfides and oxides, and not hot hydrothermal brine. (b) During the hydrothermal fluid process, new crystals formed, without occurrence of cryptocrystals or noncrystyals, needless to say immiscibility. (c) Cryptocrystals, ultra-microlite and noncrystyals usually formed as a result of rapid cooling of the melt. The immiscibility exhibited in Figs. 3a and 3d is similar to that proposed by Bea et al. (d) The coexistence of

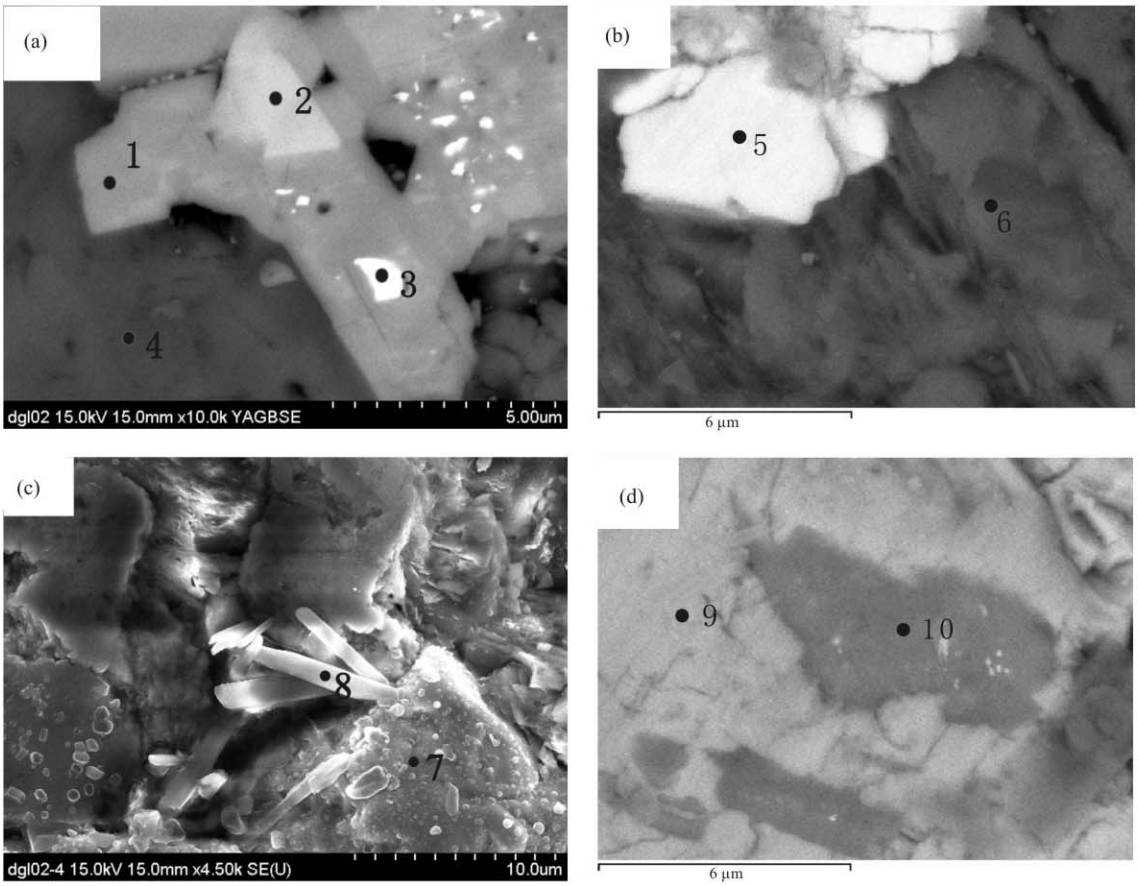

Fig. 3. SEM images showing the compositions of the BOM in altered lamprophyre (DGL-02) from the Donggualin ore block.

(a), the immiscibility relationship among rutile (1), tungstiferous rutile (2) and scheelite (3), and the precipitating cocrystallization relationship between rutile and dolomite (4); (b), the precipitating cocrystallization relationship between mispickel (5) and microcline (6); (c), the special-concomitant relationship between pyrite (7) and anhydrite (8); (d), the immiscibility relationship between gray hematite (9) and rutile (10) with the exsolution of scheelite in it.

immiscibility and precipitating cocrystallization suggests that the BOM-forming fluid has changed from the melt to the hydrothermal fluid in correspondence to the changes in physical and chemical conditions (high temperature→low temperature and a reducing environment→an oxidizing environment). Therefore, the BOM was formed during the rapid cooling of the melt. Coltorti et al. (2004) regarded the ultra-microlite glass-like material as a metasomatic agent of the alkaline magma or melt.

(3) A mantle fluid or a magmatic fluid?

Generally speaking, the magmatic fluids refer to the magma and post-magma fluids. Magma is of the ability of crystallization, and the post-magma fluid is the hydrothermal fluid excreted during magma crystallization and diagenesis processes. Obviously, the BOM-forming melt is different from the magma or post-magma fluid, but similar to the mantle fluids. This is demonstrated as follows:

Based on the researches on melt inclusions from mantle xenoliths, Andersen and Neumann (2001) observed the immiscibility among silicates, sulfides and carbonates. The experimental pressure of the melt inclusions was lower than the standard mantle pressure 1.4 Pa, and it is then concluded that melt inclusions were stretched and something contained in the inclusions might be lost. During transportation of the melt inclusions from mantle xenoliths, the HTP mantle fluid changed into one of relatively low temperature and pressure. From studies of the CO_2-bearing inclusions, silicate glass and carbonates from the amphibolite-phlogopite-spinel peridotite in Pleistocene alkaline basalts, De Stefano et al. (2009) noticed that their $\delta^{18}O$ and $\delta^{13}C$ values cannot meet the standard mantle values, and argued that it is the result of interaction between the alkaline magma and mantle xenoliths, which was caused by carbonation and the alkaline magma degassing process. During the mantle metasomatism as mentioned above, two assemblages were formed. The one is silicate glass-olivine-clinopyroxene-spinel, and the other is amphibole-phlogopite-apatite (Gregory et al., 1997). Du (1996) regarded the alkaline metasomatism as a symbol of transformation of a mantle fluid to a crustal fluid. Deduced from the above analysis, coexistence of immiscibility and precipitating cocrystallization is the result of transformation of a mantle fluid to a crustal fluid, and the metasomatic

alkaline amphibole from altered lamprophyre is an expression of mantle fluid metasomatism.

The immiscibility texture (Fig. 3d and measuring spot 9 in Table 2) from the BOM indicates that specularite resulted from the transformation of magnetite during the process when the mantle fluid changed to the crustal fluid (Liu et al., 2010). This is similar to the transformation of magnetite to specularite observed from Na-rich glass in garnet pyroxenite from the Liuhe alkaline porphyry in Yunnan.

During the process when the mantle fluid changed to the crustal fluid, on the one hand, reducible minerals in the original fluid might be precipitated by reducing their solubility (Liang et al., 2004), which could be a direct effect of the fluid action, e.g., the alkaline silicates, quartz, sulfides and carbonates contained in the BOM might be reflected as a superposition of felsic silication (Fig. 2g), sulfidation and carbonation in the ores and rocks (Figs. 2a and 2b); on the other hand, the coexistence between relatively oxidized minerals and typical reduced ones might occur, as exemplified by the association of anhydrite and pyrite (Fig. 3c), the coexistence of scheelite, rutile and dolomite (Fig. 3a), and the transformation of magnetite to specularite. Therefore, the BOM is the relics of the mantle fluid which triggered off the mineralization, while its nature and compositions suggest that the mantle fluid changed from melt®supercritical fluid®crustal hydrothermal fluid corresponding to the changes of physical and chemical environments. And it can be thus treated as a new window to the dynamic deep earth.

6 Element Geochemistry

6.1 Major oxides of the ores and rocks

The major oxide compositions of ores and rocks from the Laowangzhai gold deposit are listed in Table 3. The SiO_2 contents of altered quartz sandstone, antimony-bearing quartz porphyry, carbonaceous slate and silicated lamprophyre are higher than those of the wall rocks. The CaO, MgO, Na_2O and K_2O contents of altered ultrabasic intrusive rocks, pyritized rocks and altered olivine pyroxenite increase, indicating alteration of the rocks; while the SiO_2 content of altered lamprophyre increases, and its CaO, MgO, Na_2O and K_2O contents decrease. Deduced from the above description, the alteration and metasomatism may be constrained by the siliceous-alkaline fluid, which is favorable for migration and enrichment of ore-forming

Table 3 Chemical compositions of rocks and ores in the Laowangzhai gold deposit (%)

Serial No.	Sample No.	Rock type	SiO_2	TiO_2	Al_2O_3	Fe_2O_3	FeO	MnO	MgO	CaO	Na_2O	K_2O	P_2O_5	CO_2	SO_2	H_2O^+	H_2O^-	total
1	LWZ-01-1	Altered ultrabasic intrusive rock	40.14	0.51	17.23	2.86	3.34	0.00	8.85	12.40	2.85	0.60	0.07	0.00	0.85	8.93	0.00	98.63
2	LWZ-02-1	Pyritization altered rock	39.58	0.05	1.61	1.83	3.76	0.00	11.61	17.08	0.12	0.48	0.08	0.00	0.01	22.10	0.00	98.30
3	ZYDGL-1	Sb-bearing quartz porphyry	75.88	0.07	12.60	0.27	0.76	0.01	0.52	0.46	0.20	3.39	0.08	0.41	3.77	1.16	0.39	99.97
4	ZYDGL6-2	Altered olivine pyroxenite	27.29	0.59	9.45	2.39	3.94	0.11	8.96	16.75	0.12	2.29	0.35	21.82	4.31	0.88	0.76	100.01
5	ZYDGL-4	Lamprophyre vein	47.80	0.69	9.81	2.88	4.02	0.11	11.69	4.96	1.19	5.04	0.58	8.41	0.29	1.98	1.36	100.81
6	ZYLWZ-6-1	Lamprophyre	46.26	0.70	11.39	1.93	4.53	0.09	7.32	7.70	2.53	2.07	0.49	11.19	2.15	0.86	0.52	99.73
7	HZL**	Unweathered lamprophyre	47.35	0.67	12.12	2.34	4.03	0.14	8.32	7.29	1.63	4.39	0.57	8.62		2.01	0.21	99.69
8	W2*	Silicated lamprophyre	73.30	0.42	13.62	2.03	0.55	0.02	0.50	0.01	0.29	4.44	0.18			4.05		99.41
9	D2*	Silicated lamprophyre	88.70	0.22	5.76	0.63	0.62	0.04	0.10	0.21	0.19	1.70	0.09			1.00		99.26
10	ZYDGL6-3	Carbonaceous slate	61.00	0.31	12.42	1.77	2.41	0.08	2.53	4.66	0.17	3.53	0.13	5.39	3.88	1.15	0.37	99.80
11	LWZ-02-2	Altered quartz sandstone	76.54	0.17	2.86	1.77	3.86	0.00	1.70	4.34	0.07	0.78	0.17	0.00	0.87	4.72	0.00	97.85

Note: Data with * are from He and Hu (1996), and those with ** are average values, after Huang and Liu (1999), and tested by the Institute of Geochemistry, Chinese Academy of Sciences. The others are from this paper and tested by the Sichuan Bureau of Geology and Mineral Resources (2007).

Table 4 Trace elements of rocks and ores in the Laowangzhai gold deposit ($\times 10^{-6}$)

Sample No.	Rock type	Sr	K	Rb	Ba	Th	Ta	Ce	Zr	Hf	Ti	Yb	Sc	Cr	Ni
LWZ-03-3	Calcite vein from ores	863.45		0.06	5.70	0.21		6.25	0.14	0.01		0.71	2.27	2.78	2.65
LWZ-02-2	Altered quartz sandstone	84.99		32.26	241.73	3.66		18.23	92.87	2.48		0.88	3.52	168.82	32.42
LWZ-01-1	Altered ultrabasic intrusive rock	269.12		16.31	37.85	0.23		5.77	31.33	0.89		1.24	18.27	632.41	360.62
LWZ-01-4	Carbonaceous slate	82.49		265.37	682.83	18.54		91.32	142.32	4.07		3.14	20.65	99.80	30.47
LWZ-02-1	Pyritization altered rock	935.10	5078.30	32.30	1760.90	0.28	0.02	3.21	9.30	0.46	665.60	0.28	6.53	2116.10	502.95
LWZ-03-1	Carbonaceous gold ore	32.79	13965.32	92.50	479.90	4.80	0.45	27.62	58.90	1.71	2050.00	1.89	7.20	91.80	31.00
YG-41*	Quartz porphyry	153.00	39800.00	86.40	478.00	9.71	2.98	79.43	32.00	2.05	1000.00	2.44	10.50	25.00	9.87
YD-20*	Lamprophyre	1049.00	30600.00	140.00	2602.00	11.10	0.73	98.52	109.00	4.82	4100.00	1.56	27.30	521.00	365.00
YD-62*	Silicated lamprophyre	380.00	34200.00	115.00	418.00	7.32	0.32	49.50	57.10	3.14	2424.00	1.76	27.30	283.00	84.00

Note: Data with * are from He and Hu (1996); the others are from this paper. The rocks and veins are tested by the State Key Laboratory of Geological Processes and Mineral Resources, China University of Geosciences (2007), and the ores by the Quality Supervision Center of Exploration Geochemistry, Ministry of Land and Resources (2007).

elements.

6.2 Trace element geochemistry of ores and rocks

The trace element data and distribution patterns of ores and rocks from the Laowangzhai gold deposit are given in Table 4 and Fig. 4. The Sc, Cr and Ni contents in the calcite vein, silicated quartz vein, wall rocks and ores are lower than the primitive mantle values, while the LILEs are enriched. The average contents of all these elements are similar except the diversity in Sr, Ba and Zr contents. And, except the altered ultrabasic intrusive rocks, pyritized rocks and the calcite vein, Th and Ta are enriched while Cr and Ni are depleted, which indicates that the ore-forming fluid was derived from enriched mantle and overlapped by crustal fluids, which triggered off the depletion of incompatible elements and LILEs, while the mantle fluid metasomatism brought out the enrichment of LREEs, incompatible elements and HFSEs (Liu et al., 2003, 2009). Through researches on the element geochemistry of ores and rocks from the Laowangzhai and Dongguanlin ore blocks, we have acquired a simple but clear understanding about the geochemical dynamics of mantle-crustal overprint during the ore-forming process.

6.3 Rare earth element geochemistry of the ores and rocks

The rare earth element data and major characteristic parameters of the ores and rocks from the Laowangzhai gold deposit are listed in Table 5. SREE varies widely, and that of veins is the lowest. LREE changed from 1.92 to 220.43×10^{-6}, HREE from 0.33 to 23.86×10^{-6}, and LREE/HREE varied from 0.78 to 13.79. Deduced from the REE chondrite-normalized pattern of the samples given in Figs. 5 to 7, from veins→wall rocks→ores, δEu varies from $+\delta$Eu→weak $-\delta$Eu→strong $-\delta$Eu, while δCe changes from normal→weak $-\delta$Ce.

As exhibited in Fig. 5, the calcite vein from the Laowangzhai ore block, the primitive vein and the calcite vein from the Dongguanlin ore block show $+\delta$Eu, while the late-stage silicated quartz vein from the Dongguanlin ore block has no δEu or δCe anomaly. The trends of increasing δEu from veins→wall rocks→ores suggest that the ore-forming fluid has changed from high temperature to low temperature, and from a reducing to an oxidizing environment.

During the ore-forming process, mantle fluids were overprinted by crustal fluids, resulting in changes of δEu from $+\delta$Eu to $-\delta$Eu. The $-\delta$Eu is a symbol for hydrothermal transformation and mantle-crustal overprint (Xu et al., 1997). Reverse trends of δEu and δCe can be taken as signs of the mantle-crustal overprint intensity.

Based on the above discussions, it is concluded that the ore-forming elements or fluids are not predominantly

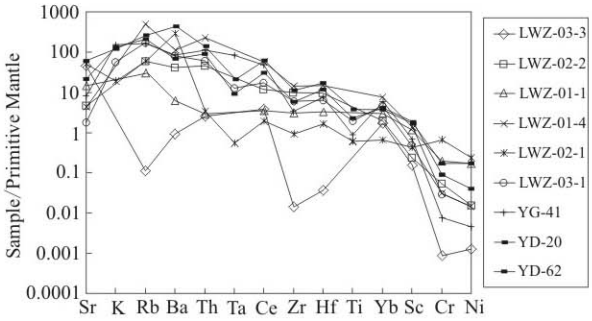

Fig. 4. Distribution patterns of trace elements of ore rocks in the Laowangzhai gold deposit.
The sample numbers are the same as in Table 2.

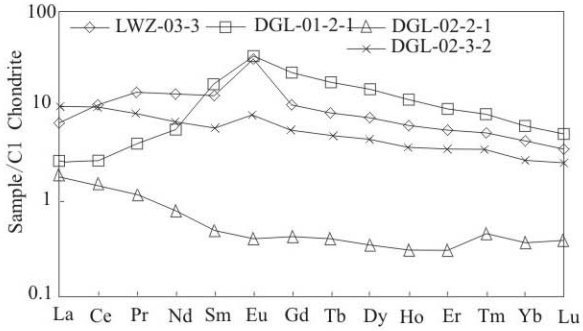

Fig. 5. Chondrite normalized REE distribution patterns of quartz and calcite veins in the Laowangzhai gold deposit.
LWZ-03-3, calcite vein (in ores); DGL-02-2-1, protogene silicated quartz vein; DGL-02-2-2, late-stage silicated quartz vein; DGL-02-3-2, calcite vein (in ores).

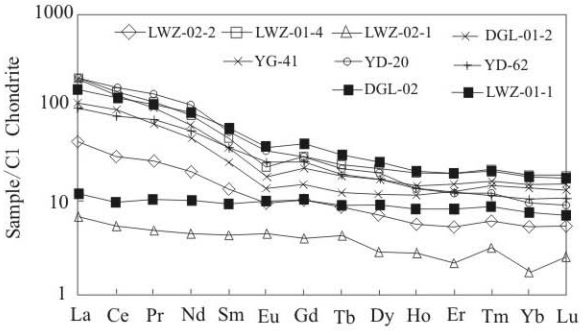

Fig. 6. Chondrite normalized REE distribution patterns of country rocks in the Laowangzhai gold deposit.
LWZ-02-2, carbonatized quartzose sandstone; LWZ-01-4, carbonaceous slate; LWZ-01-1, (serpentine) altered hyperbasite intrusive rock; LWZ-02-1, pyritization altered rock; DGL-02, altered lamprophyre (with quartz peritecticum); DGL-01-2, carbonaceous phyllite; YG-41, granite porphyry*; YD-20, lamprophyre*; YD-62, mineralized lamprophyre* (* data from Huang and Liu, 1999).

provided by the wall rocks or strata, but controlled by the LREE-rich mantle fluid which was later overlapped by crustal hydrothermal fluid. Partial melting of the primitive mantle has led to the depletion of basaltic compositions and incompatible elements, especially the LILEs, while the mantle fluid metasomantism has resulted in the enrichment of LREEs, incompatible elements and highly siderophile elements. Based on the element geochemical

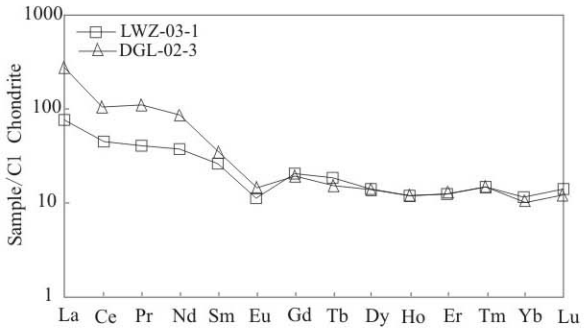

Fig. 7. Chondrite normalized REE distribution patterns of carbonic ores in the Laowangzhai gold deposit.
LWZ-03-1, carbonaceous ores in the gold deposit; DGL-02-3, carbonaceous ores in the gold deposit.

studies of the rocks, ores and veins from the Laowangzhai gold deposit, it is proved that deep geologic processes and mantle-crustal contamination are the geochemical dynamics of the ore-forming process.

7 Discussions

Studies have shown that the ore-forming fluid of the Laowangzhai gold deposit was derived from the mantle. The $\delta^{34}S$ values of stibnite, pyrite and arsenopyrite changed from −2.22‰ to +2.27‰ with a peak at 4.99‰, suggesting that S came from the mantle (He and Hu, 1996). $\delta^{13}C$ of calcite from the gold ores varying from −7.00‰ to −2.70‰ exhibited a strong magmatic feature. The H and O isotopes of the ore-forming fluid showed that it belonged to the Au-Cu-Fe-Co primitive magmatic fluid (He and Hu, 1996; Bian et al., 1998), while its Pb isotope exhibited a mantle-crustal overprint feature (Zhang et al., 2010).

Based on the noble gas isotope studies, Hu and Tang (1996) proved that mantle He accounted for about 11%-52% of the total. This result is in accordance with our research that the ore-forming fluid was derived from the mantle. Most of the endogenic ore deposits are related to the deep geological fluid (Mao et al., 2005) reckoned to be a trans-magmatic fluid by Luo et al. (2007, 2008). In terms of the trans-magmatic fluid theory (Luo et al., 2007, 2008), the ore-forming fluid system can be independent of the magma system. Relationships between the two are classified into three types: (1) The ore-forming fluid was well trapped in the magma body, forming an orthomagmatic ore deposit; (2) part of the ore-forming fluid escaped from the magma body and flowed to the wall rocks, forming a contact or skarn ore deposit; (3) the ore-forming fluid escaped from the magma body totally, and flowed along the faults, resulting in high temperature→mesothermal temperature→low temperature hydrothermal ore deposits. The composite metallogenesis effects of the mantle fluid consisted of the melt or magma from the mantle, the supercritical fluid and related hydrothermal fluid (Liu et al., 2010). The mantle fluid process can be divided into two steps: (1) Mantle metasomatism, which refers to the metasomatism process caused by mantle degassing, and alkaline magma was formed in the enriched mantle; (2) mantle fluid metasomatism, referring to the metasomatism process triggered off by the fluid derived from the enriched mantle, which is named the mantle fluid. The mantle fluid may be independent of the magma system and changed from melt→supercritical fluid→hydrothermal fluid, which is favorable for the formation of various ore deposits.

Based on the above analysis, it can be deduced that the BOM from altered lamprophyre is the result of rapid cooling of the upwelling mantle fluid, during which process the temperature, pressure and oxygen fugacity changed, the mantle fluid was transformed from a melt to a hydrothermal fluid, and the coexistence of immiscibility and precipitating cocrystallization occurred. At the mean time, the unconsolidified mantle fluid escaped from the lamprophyre, moved along the faults and fractures altered the wall rocks with carbonation, silication and sulfidation developed. Combined with the geological backgrounds, it is reasonable to infer that deep faults and secondary faults played an important role in the mantle fluid transportation and mineralization.

8 Conclusions

(1) The coexistence of immiscibility and precipitating cocrystallization in the BOM from altered lamprophyre suggests that the BOM is a trace or relict of the mantle fluid during the ore-forming process. It is the mantle fluid that triggered off mantle-crustal overprint, and provided part of the ore-forming materials and energy.

(2) The altered wollastonite from pyroxene peridotite can be regarded as an indicator that high-temperature recombination reaction of siliceous carbonate melts occurred in the alteration process, which implied that the ore-forming fluid is a kind of mantle fluid that triggered off the mantle-crustal overprint.

(3) The changes of major oxides exhibited as increases of silication and alkaline elements, which is favorable for the gold formation. The enrichment of LILEs, incompatible elements and HSFEs constituted an implication of the mantle-crustal overlap. The reverse evolution of δEu and δCe from the ores and rocks can be regarded as an indicator of participation of the mantle fluid in mineralization in the crust, which incurred the mantle-crustal contamination.

(4) The ore-forming fluid and mineralizing materials of

the Laowangzhai gold deposit were derived partly from the mantle, and the mantle-crustal overprint in particular played an important role in the ore-forming process.

Acknowledgements

The study is jointly supported by the National Natural Science Foundation of China (Grants No. 40473027 and 40773031), the Foundation of Doctoral Supported by the Ministry of Education (20105122110010 and 20115122110005), the Foundation of Open Subjects of State Key Laboratory for Mineral Deposits Research, Nanjing University (14-08-3), the Project of the State Key (Preparation Support) Disciplines of Mineralogy, Petrology and Mineral Deposit Geology of Sichuan Province (SZD0407), and the authors are indebted to the academic suggestions from two anonymous experts, whose advice and encouragement have improved the quality of this paper.

Manuscript received Mar. 2, 2012
accepted Apr. 18, 2012
edited by Zhu Xiling

References

Andersen, T., and Neumann, E.R., 2001. Fluid inclusions in mantle xenoliths. *Lithos*, 55(1–4): 301–320.

Bea, F., Arzamastsev, A., and Montero, P., 2001. Anomalous alkaline rocks of Soustov, Kola: Evidence of mantle-derived metasomatic fluids affecting crustal materials. *Contributions to Mineralogy and Petrology*, 140(5): 554–566.

Bian Qiantao, 1998. Explore the relationship between the texture structure of crust-mantle and the Laowangzhai ultralarge gold deposit. *Science in China* (Series D), 28(4): 303–309 (in Chinese).

Cao Shuyun, Li Junlai, Bernd Leiss and Zhao Chunqiang, 2010. New Zircon U-Pb Geochronology of the Post-kinematic Granitic Plutons in the Diancang Shan Metamorphic Massif along the Ailao Shan-Red River Shear Zone and Its Geological Implications. *Acta Geologica Sinica* (English edition), 84(6): 1474–1487.

Chen Jianlin, Xu Jifeng, Wang Baodi and Kang Zhiqiang, 2010. Geochemistry of the Eocene Felsic Porphyric Rocks and High-Mg Potassic Rocks along JARSZ: Implication for the Tectonic Evolution in Eastern Tibet. *Acta Geologica Sinica* (English edition), 84(6): 1448–1460.

Coltorti, M., Beccaluva, L., Bonadiman, C., Faccini, B., Ntaflos, T., and Siena, F., 2004. Amphibole genesis via metasomatic reaction with clinopyroxene in mantle xenoliths from Victoria Land, Antarctica. *Lithos*, 75(1–2): 115–139.

De Stefano, A., Rivalenti, G., Preite-martinez, M., Scambelluri, M., and Vannucci, R., 2009. CO_2 fluid and silicate glass as monitors of alkali basalt/peridodite interaction in the mantle wedge beneath Gobernador Gregores, Southern Patagonia. *Lithos*, 107(1–2): 121–133.

Ding Qingfeng, 2001. Advances in lamprophyre study. *World Geology*, 20(1): 17–24 (in Chinese).

Du Letian, 1996. The relationship between crust fluids and mantle fluids. *Earth Science Frontier*, 3(3–4): 172–180 (in Chinese).

Gregory, M.Y., Kamenetsky, V., David, H.G., and Trevor, J.F., 1997. Glasses in mantle xeneliths from western Victoria, Australia, and their relevance to mantle processes. *Earth and Planetary science Letters*, 148(3–4): 433–446.

Hao Tianyao, Jiang Weiwei, Xu yi, Qiu Xuelin, Liu Jianhua, Dai Minggang, Xu Ya, Huang Zhongxian and Song Haibin, 2005. Geophysical research on deep structure feature in study region of Red River fault zone. *Progress in Geophysics*, 20(3): 584–593 (in Chinese).

He Mingyou and Hu Ruizhong, 1996. Deep fluid—one probability for the sources of ore-bearing in the Laowangzhai gold deposit. *Geology Geochem*istry, (2): 27–31 (in Chinese).

He Wenju, 1993. Characteristic of the lamprophyre and the relation with gold mineralization in Zhenyuan gold mine field. *Yunnan Geology*, 12(2): 148–158 (in Chinese).

Hu Yunzhong and Tang Shangchun, 1995. *Geology of Gold Deposits in Ailaoshan*. Beijing: *Geological Publishing House*, 134–219 (in Chinese).

Huang Zhilong, 2001. Degassing in the processes of mantle-derived magmatism: As exemplified by lamprophyres in the Laowangzhai gold deposit, Yunnan Province. *Bulletin of Mineralogy, Petrology and Geochemisty*, 20(1): 1–5 (in Chinese).

Huang Zhilong and Liu Congqiang, 1999. *The Genesis of Lamprophyres and Its Relation of It to Mineralization in the Laowangzhai gold deposit Area, Yunnan*. Beijing: Geological Publishing House, 82–97 (in Chinese).

Huang Zhilong and Wang Liankui, 1996. Geochemistry of lamprophyres in the Laowangzhai gold deposit, Yunnan Province. *Geochimica*, 25(3): 255–263 (in Chinese).

Huang Zhilong, Wang Liankui and Liu Jun, 1997. Compositional modeling of mantle source for lamprophyres in the Laowangzhai gold orefield, Yunnan. *Acta Mineralogica Sinica*, 17(3): 316–320 (in Chinese).

Huang Zhilong, Wang Liankui and Zhu Chengming, 1996. The regularities of element activities in alteration of lamprophyres in Zhenyuan gold deposits, Yunnan Province. *Geotectonica et Metallogenia*, 20(3): 245–254 (in Chinese).

Hou Zengqian, Pan Guitang, Wang Anjian, Mo Xuanxue, Tian Shihong, Sun Xiaoming, Ding Lin, Wang Erqi, Gao Yongfeng, Xie Yuling, Zeng Pusheng, Qing Kezhang, Xu Jifeng, Qu Xiaoming, Yang ZhiMing, Yang Zhusen, Fei Hongcai, Meng Xiangjin and Li Zhenqing. 2006. Metallogenesis in Tibetan collisional orogenic belt: II. Mineralization in late-collisional transformation setting. *Mineral Deposits*, 25(5): 521–543 (in Chinese).

Li Xianhua and Sun Xianshu, 1995. Lamprophyre and gold mineralization—An assessment of observations and theories. *Geological Review*, 41(3): 252–260 (in Chinese).

Liang Huaying, Xie Yingwen, Zhang Yuquan and Ian, C., 2004. Controlling of forming and evolution of kalium-rich alkalic body on Cu mineralizing—example for Machangqing Cu deposit. *Progress in Natural Science*, 14(1): 116–120 (in Chinese).

Liang Yeheng, Sun Xiaoming, Shi Guiyong, Hu Beiming, Zhou Feng, Wei Huixiao and Mo Ruwei, 2011. Ore-forming fluid geochemistry and genesis of Laowangzhai large scale

orogenic gold deposit in Ailaoshan gold belt, Yunnan Province, China. *Acta Pertrologica Sinica*, 27(9): 2533–2540 (in Chinese).

Liu Xianfan, Cai Yongwen, Lu Qiuxia, Tao Zhuan, Zhao Fufeng, Cai Feiyue, Li Chunhui and Song Xiangfeng, 2010. Actual traces of mantle fluid from alkali-rich porphyries in western Yunnan, and associated implications to metallogenesis. *Earth Science Frontiers*, 17(1): 114–136 (in Chinese).

Liu Xianfan, Liu Jiaduo, Zhang Chengjiang, Wu Dechao, Li Youguo and Yang Zhengxi, 2003. Study of elements geochemistry characteristics for ultramafic deep xenoliths in alkali-rich porphyry. *Mineralogy and Petrology*, 23(3): 39–43 (in Chinese).

Liu Xianfan, Zhao Fufeng, Tao Zhuan, Song xiangfeng, Cai Yongwen and Cai Feiyue, 2009. Mantle fluid metasomatism in Jinhe intrusive body of Jianchuan, Yunnan Province, and its ore-forming implication. *Mineral Deposits*, 28(2): 185–194 (in Chinese).

Luo Zhaohua, Lu Xinxiang, Guo Shaofeng, Sun Jing, Chen Bihe, Huang Fan and Yang Zongfeng, 2008. Metallogenic systems on the transmagmatic fluid theory. *Acta Petrologica Sinica,* 24 (12): 2669–2678 (in Chinese).

Luo Zhaohua, Mo Xuanxue, Lu Xinxiang, Chen Bihe, Ke Shan, Hou Zengqian and Jiang Wan, 2007. Metallogeny by trans-magmatic fluids—theoretical analysis and field evidence, *Earth Science Frontiers*, 14(3): 165–183 (in Chinese).

Lü Boxi, 1994. The new magmatite feature and genesis of the Laowangzhai gold deposit, Zhenyuan county (Donggualin deposit included), Yunnan. *Yunnan Geological Science and Technology Infor*mation, (1): 1–12 (in Chinese).

Mao Jingwen, Li Xxiaofeng, Zhang Ronghua, Wang Yitian, He Ying and Zhang Zuoheng, 2005. *Deep-Derived Fluid-Related Ore-Forming System.* Beijing: China Land Press, 1–365 (in Chinese).

Ren Shengli, Qin Gongjiong, Chi Sanchuan and Tan Shangchun., 1995, Au origin of Laowangzhai-Donggualin gold deposit, Zhenyuan County, Yunnan Province. *Earth Science* (Journal of China University of Geosciences), 20(1): 47–52 (in Chinese).

Tang Shangchun, Li Jingdian and He Shuxin, 1991. On metallogenic regularity of gold metallogenic belts in northern section of Ailao Mountain. *Yunnan Geology*, 10 (1): 44–69 (in Chinese).

Wang Jianghai, Qi Liang, Yin An and Xie Guanghong, 2001. Platinum family element geochemistry and invasion age of lamprophyre from the Laowangzhai gold deposit in Yunnan Province, China. *Science in China* (Series D), 31(Sup.): 122–127.

Xu Xueyi, Huang Yuehua, Xia Linqi and Xia Zuchun, 1997. Phlogopite amphibole pyroxenite Xenoliths in Langao, Shaanxi Province: Evidences for mantle metasomatism. *Acta Petrologica Sinica*, 13(1): 1–13 (in Chinese).

Xue Chuandong, Liu Xing, Tan Shucheng and Qin Dexian, 2002. Typomorphic characteristics of main minerals from the Laowangzhai gold deposit, western Yunnan. *Mineralogy and Petrology*, 22(3): 10–16 (in Chinese).

Ying Hanlong and Liu Bingguang, 2000. The trace element and isotope composition and their restriction on the origin mineralization matter of Laowangzhai gold ore deposit, Yunnan. *Gold Science and Technology*, 8(2): 15–20 (in Chinese).

Zhang Jiwu, Wu Jun, Li Changshou, Su Xiaojing and Wang Junping, 2010. Geological features and genesis of the Laowangzhai gold deposit in Zhenyuan county. Yunnan. *Gold*, 31(6): 19–23 (in Chinese).